9-1-1997

Faint Sources in the EUVE Survey: Identification of White Dwarfs, Active Late-Type Stars, and Galactic Nuclei

Elisha Polomski
University of Florida

Stephane Vennes
University of California - Berkeley

John R. Thorstensen
Dartmouth College

Mihalis Mathioudakis
Queen's University Belfast

Emilio E. Falco
Harvard-Smithsonian Center for Astrophysics

THE ASTROPHYSICAL JOURNAL, 486:179–196, 1997 September 1

FAINT SOURCES IN THE *EUVE* SURVEY: IDENTIFICATION OF WHITE DWARFS, ACTIVE LATE-TYPE STARS, AND GALACTIC NUCLEI

ELISHA POLOMSKI
Department of Astronomy, 211 Bryant Space Science Center, University of Florida, Gainesville, FL 32611; elwood@astro.ufl.edu

STÉPHANE VENNES
Center for EUV Astrophysics, 2150 Kittredge Street, University of California, Berkeley, CA 94720-5030; vennes@cea.berkeley.edu

JOHN R. THORSTENSEN
Department of Physics and Astronomy, 6127 Wilder Laboratory, Dartmouth College, Hanover, NH 03755; thorsten@dartmouth.edu

MIHALIS MATHIOUDAKIS
Department of Pure and Applied Physics, Queen's University of Belfast, Belfast BT7 1NN, Northern Ireland, UK; M.Mathioudakis@qub.ac.uk

AND

EMILIO E. FALCO
Harvard-Smithsonian Center for Astrophysics, Optical and Infrared Astronomy Division, MS 19, 60 Garden Street, Cambridge, MA 02138; falco@cfa.harvard.edu

Received 1996 November 18; accepted 1997 April 7

ABSTRACT

We report the classification of 21 new extreme-ultraviolet sources from the recent catalog of Lampton et al. The optical spectra presented identify the objects as 14 active late-type stars (including two double active stars and a possible T Tauri star), three white dwarfs, and six active galactic nuclei (a Seyfert galaxy, the BL Lac object 1ES 1028+511 [=EUVE J1031+508], and four quasi-stellar objects). We have detected Ca II absorption lines in the BL Lac object and measured its redshift. Two of the white dwarfs are unusually massive ($M > 1.1\ M_{\odot}$). Our sample of late-type stars includes five previously known high proper motion objects (EUVE J1004+503, J2244−332A,B, J1802+642, and J1131−346), of which one is the well-known flare star TX PsA (EUVE J2244−332B). We report an unusually high level of activity for the primary component of the TX PsA system (EUVE J2244−332A), which may indicate flare activity. The group of late-type stars is on average almost 3 mag fainter ($\langle m \rangle \approx 13$) than the typical member of the *Extreme Ultraviolet Explorer* (*EUVE*) all-sky survey catalog. All Galactic and extragalactic objects were also detected in the *ROSAT* Position Sensitive Proportional Counter survey, and most are at the faint limit of the *EUVE* detectors. These new identifications substantially increase the total number of EUV-selected extragalactic sources.

Subject headings: galaxies: active — stars: activity — stars: late-type — ultraviolet: stars — white dwarfs — X-rays: stars

1. INTRODUCTION

Until relatively recently (Lampton et al. 1976), the high opacity of the interstellar medium at extreme-ultraviolet wavelengths ($\lambda < 912$ Å) was thought to preclude the detection of most astrophysical sources. The launch of the *Extreme Ultraviolet Explorer* (*EUVE*) in 1992, with detectors spanning the 50–740 Å bandpass, initiated the first thorough exploration of this heretofore opaque region of the spectrum. During the 6 month survey phase, exposure times for sources in the scan path varied because of the specific geometry of the survey; exposure time ranged from 400 s at the ecliptic equator to 20,000 s at the poles. Additional details concerning the *EUVE* survey have been presented by Bowyer et al. (1996).

With completion of the *EUVE* all-sky survey in 1993 July, nearly a thousand EUV sources are now known (exactly 918, combining the Lampton et al. 1997 and Bowyer et al. 1996 catalogs). Lampton et al. (1997) still report 76 unidentified sources at the faint limit of the EUV detectors, a list that may include some variable sources. Almost 60% of the sources discovered during the *EUVE* survey are stars with convective envelopes (spectral type F or later); the second most numerous class of objects are white dwarfs; extragalactic sources constitute only a small percentage of the total. If the same statistics apply to the unidentified sources, one would expect a large percentage of them to be late-type stars.

We have performed spectroscopy on the fields surrounding 21 of these faint EUV sources and have subsequently identified the objects as six active galactic nuclei (AGNs), 14 late-type stars (10 single and two double active stars), and three white dwarf stars. Finding charts are presented in Figure 1. We also obtained direct imaging of the host galaxy of one of the AGNs (EUVE J0736+257) and have detected the spatial extension of this object. In this paper, we present the optical spectra, as well as the *EUVE* and *ROSAT* Position Sensitive Proportional Counter (PSPC) count rates, for these sources. We derive distances, luminosities, and spectral types for the stellar objects. We also measure redshifts and present preliminary energy diagrams for the AGNs.

2. OBSERVATIONS AND DATA REDUCTION

All objects were initially detected by *EUVE* in the all-sky survey mode, using the Lexan detector (58–174 Å). Lampton et al. (1997) performed a cross-correlation of faint

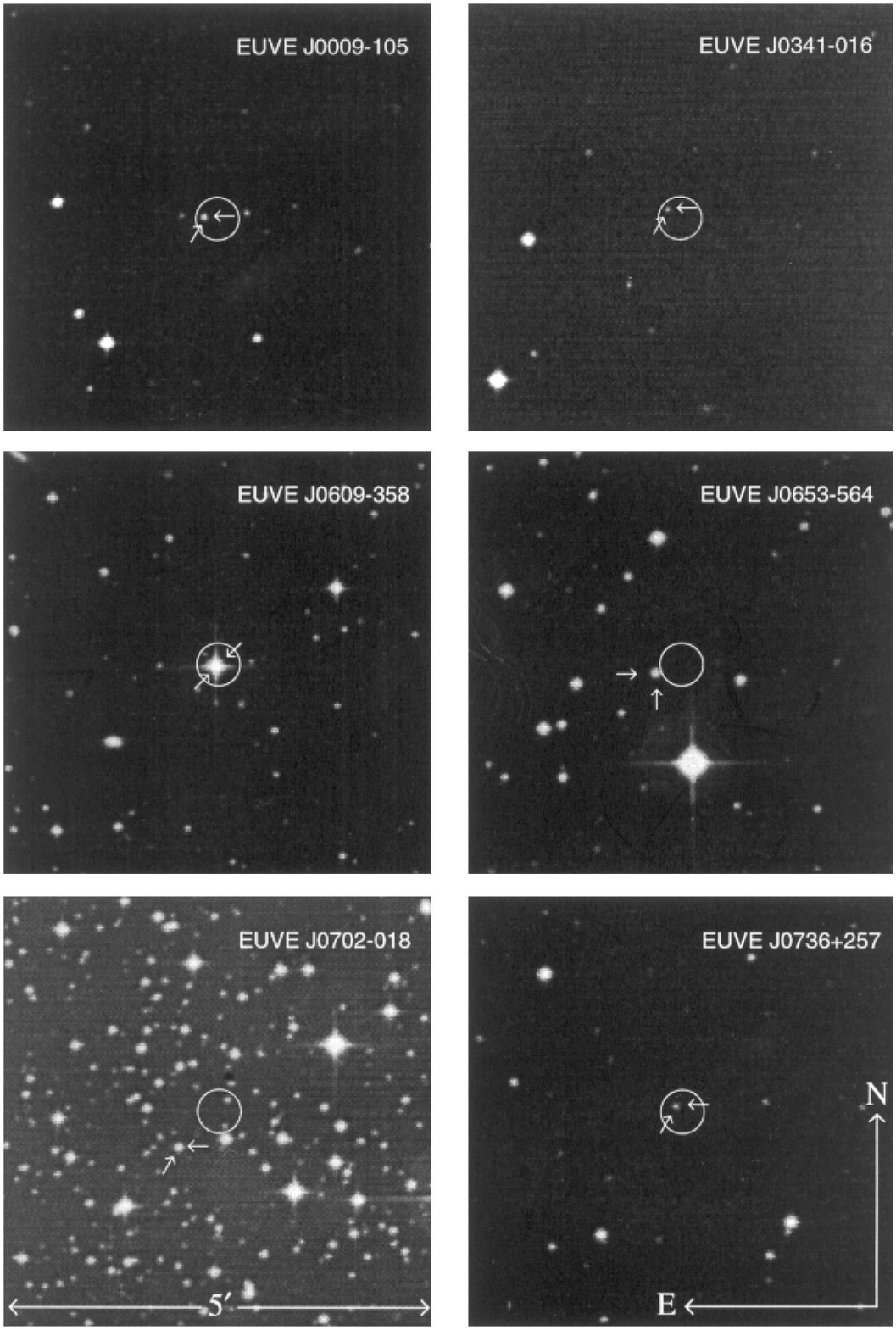

FIG. 1.—Finding charts for the 21 *EUVE*/*ROSAT* detected objects (including two double active stars). An error circle of 30″ diameter has been superposed on the images. The fields are 5′ square, and orientation is indicated on each page (north is up and east is left).

EUVE sources with the *ROSAT* PSPC catalog (5–124 Å) to verify the EUV detections. *ROSAT* and *EUVE* count rates for our objects are presented in Tables 3, 6, and 7 below. Very recently, the first *ROSAT* All-Sky Survey (RASS) catalog became available (Voges et al. 1997); Table 1 presents corroborating data from this catalog. The *ROSAT* PSPC count rates from Lampton et al. (1997) and Voges et al. generally agree; the hardness ratio HR1, defined as $(B - A)/(B + A)$, where A is the count rate between 0.1 and 0.4 keV and B is the count rate between 0.5 and 2.0 keV,

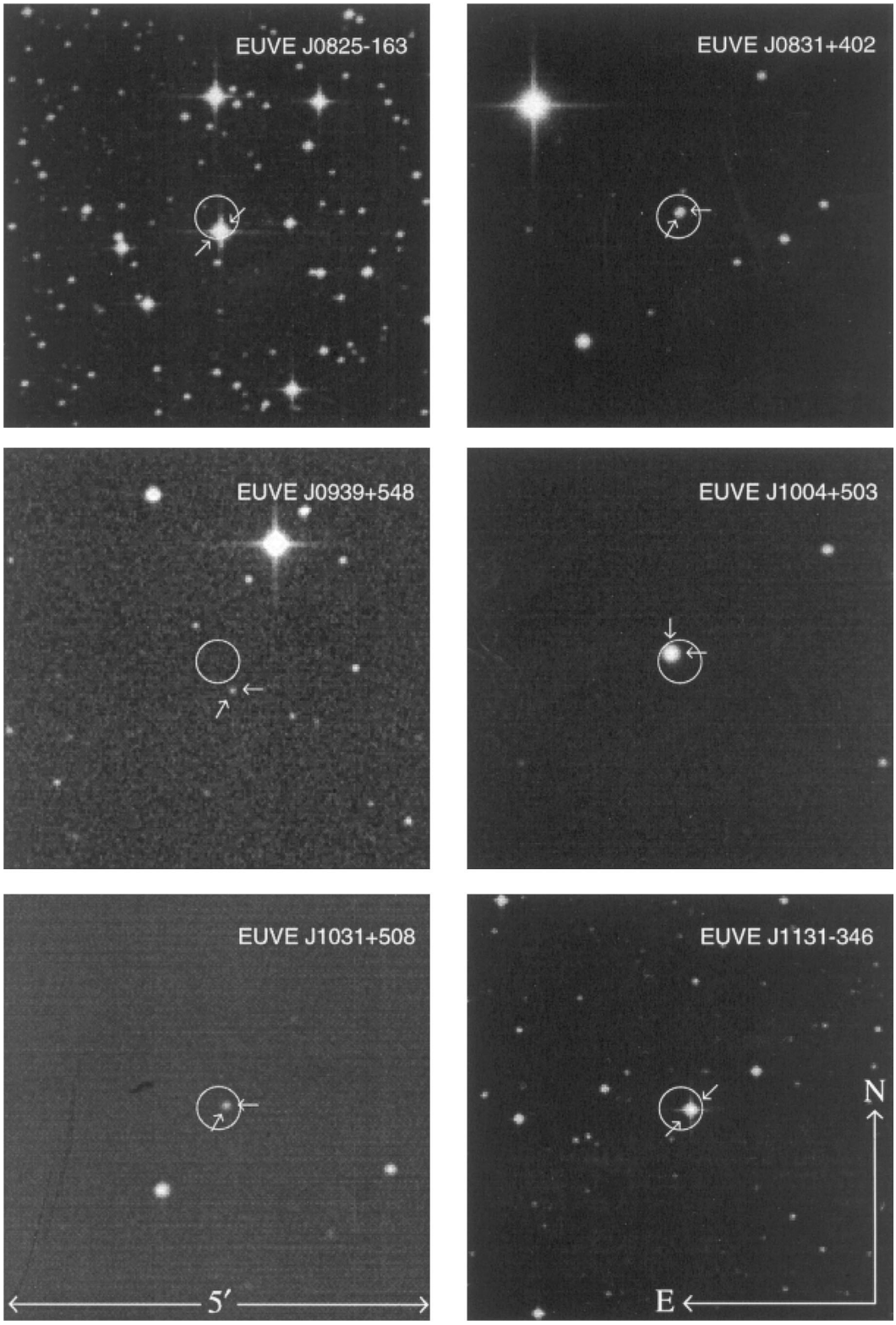

FIG. 1—*Continued*

helps discriminate between soft sources (HR1 = −1), such as white dwarfs, and hard sources (HR1 = +1), such as late-type stars and AGNs.

2.1. *Spectroscopy and Imaging*

Optical spectroscopy was performed at the Michigan-Dartmouth-MIT Observatory (MDM) 2.4 m Hiltner Telescope at Kitt Peak on 1996 January 6–12 and April 6 and 9, and at the Mount Stromlo Observatory (MSO) 74 inch (1.9 m) telescope on 1996 April 18, 19, 20, 23, and 25. During the January run at MDM, we used the Mark III spectrograph and a Tektronix 1024 × 1024 CCD with wavelength coverage between approximately 3600 and 6000 Å at 2.32 Å pixel^{-1}. The slit width was adjusted to exceed the seeing at 2″.4. During the April run at MDM, we used the Modular

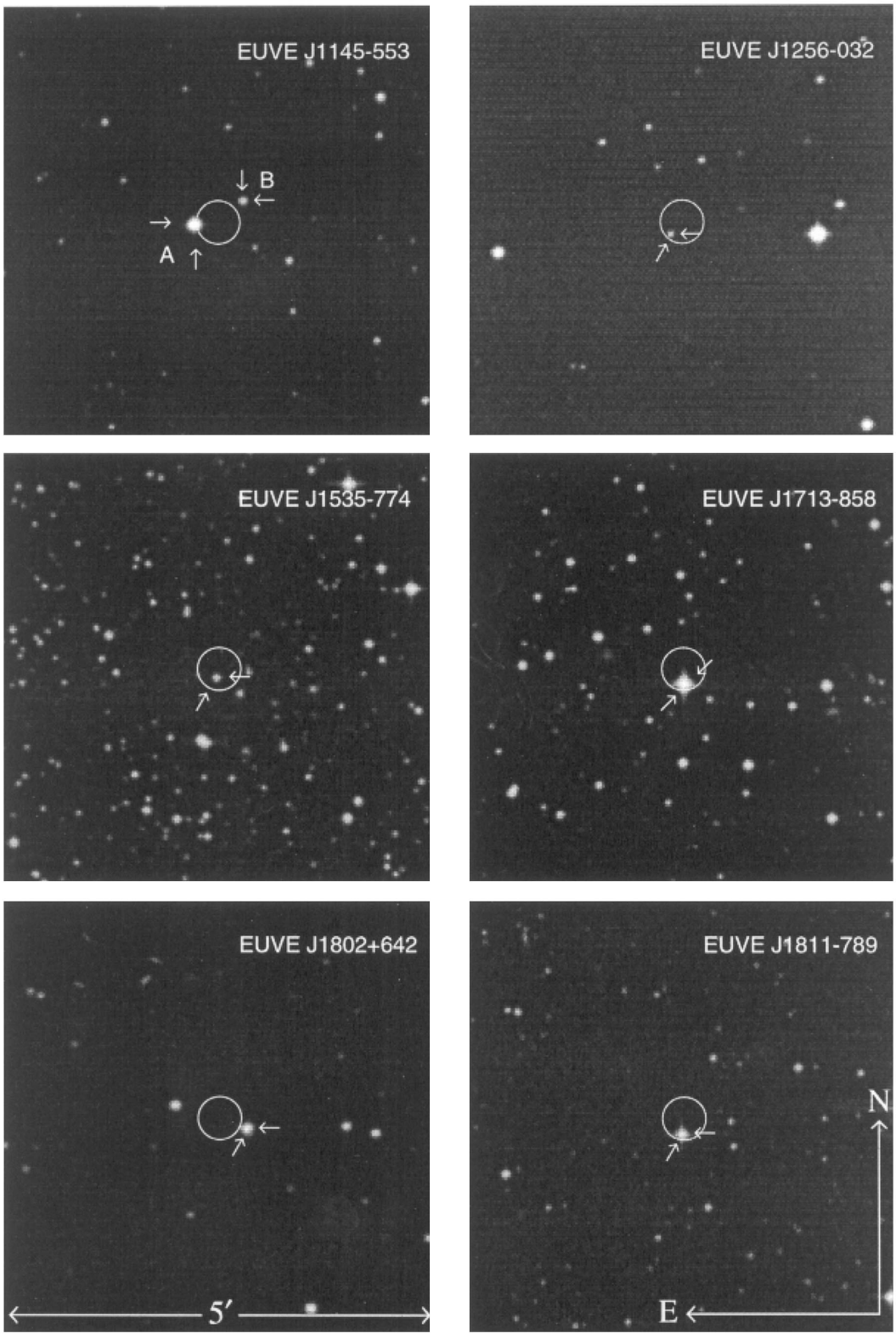

FIG. 1—*Continued*

Spectrograph and a Loral 2048 × 2048 CCD with wavelength coverage between 4200 and 6770 Å at 1.27 Å pixel^{-1}. Spectral resolution was 5–6 Å in January and 2–3 Å in April. We used Hg-Ne and Xe lamps for wavelength calibration. All spectra were bias-subtracted, flat-fielded, extinction-corrected, and wavelength- and flux-calibrated using NOAO's IRAF at the Center for EUV Astrophysics and Dartmouth College. We found that corrections for extinction critically affected the colors for observations made at large air mass.

At Mount Stromlo, two sets of instrumentation were used: a Cassegrain focus spectrograph with a 300 line mm^{-1} grating with a UVAR thinned SITe 1752 × 532 CCD, and an identical setup with a 416 × 578 GEC CCD.

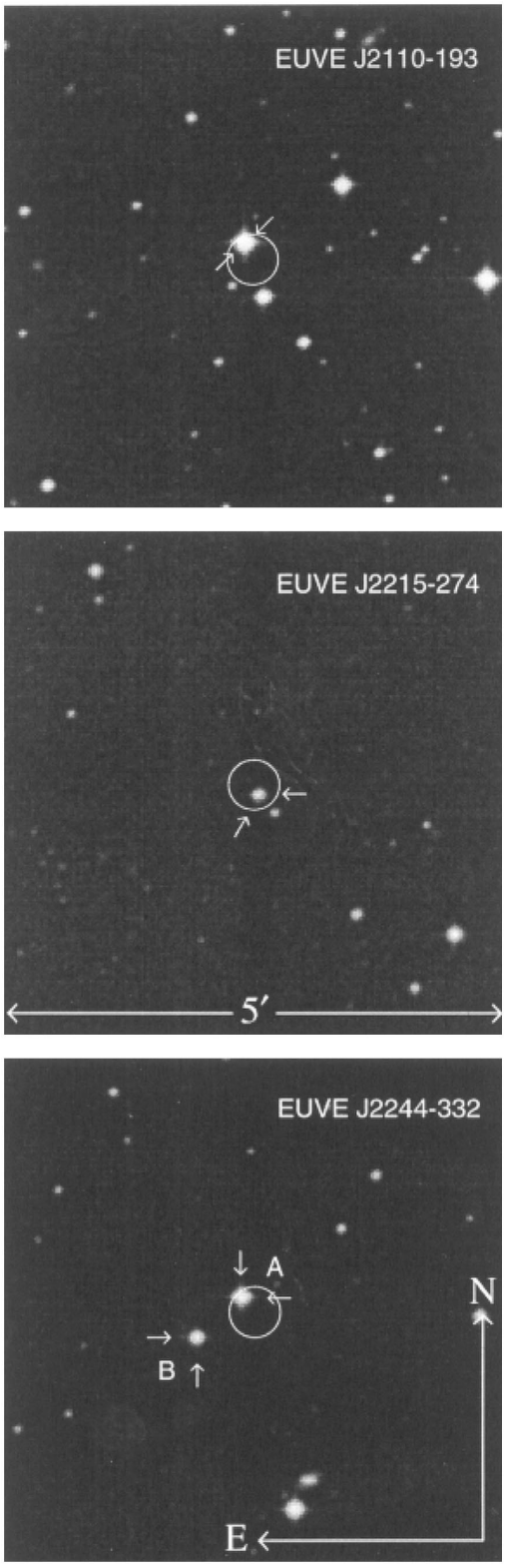

FIG. 1—*Continued*

The slit width was set at 3″. The MSO UVAR spectra cover the wavelength range from 3660 to 6040 Å at 2.72 Å pixel^{-1} for a 5–6 Å resolution while the MSO GEC spectra cover only from 3820 to 5000 Å at 2.04 Å pixel^{-1} and resolution of ≈ 6 Å.

R-band imaging of one of our targets (EUVE J0736+257) was also performed on the 2.4 m telescope at MDM. We used the Tek CCD with a Kron-Cousins *R* filter. The observation log for all four instruments is presented in Table 2.

2.2. *Magnitudes and Colors*

To find apparent magnitudes and colors, we used (1)

TABLE 1

CORRESPONDENCE BETWEEN THE LAMPTON ET AL. AND VOGES ET AL. CATALOGS

Name (EUVE)	Lampton et al. (counts s^{-1})	RASS (counts s^{-1})	Error (counts s^{-1})	Hardness Ratio (HR1)	Error
J0009−105	0.07	0.085	0.020	0.13	0.24
J0341−016	0.02	...	...	...	...
J0609−358	0.42	0.367	0.024	−0.16	0.06
J0653−564	0.07	...	...	...	...
J0702−018	0.02	...	...	...	...
J0736+257	0.07	0.066	0.015	0.34	0.23
J0825−163	0.52	0.509	0.043	−0.25	0.08
J0831+402	0.13	0.116	0.026	0.39	0.22
J0939+548	0.05	...	...	...	...
J1004+503	0.70	0.689	0.043	−0.26	0.05
J1031+508	4.66	4.464	0.092	−0.26	0.02
J1131−346	0.70	0.656	0.076	−0.31	0.29
J1145−553B	0.51	0.456	0.043	−0.07	0.09
J1256−032	0.07	0.065	0.019	−0.40	0.21
J1535−774	0.58	0.049	0.05	−1.00	0.04
J1713−858	0.18	0.204	0.034	−0.28	0.15
J1802+642	0.17	0.144	0.004	−0.19	0.02
J1811−789	0.46	0.418	0.059	0.03	0.13
J2110−193	0.37	0.440	0.043	−0.01	0.10
J2215−277	0.35	0.31	0.04	−1.00	0.02
J2244−332A,B.....	0.89	1.048	0.064	−0.23	0.05

NOTES.—Shown is a comparison between PSPC count rates from Lampton et al. 1997 and the *ROSAT* All-Sky Survey (RASS) catalog of Voges et al. 1997. The hardness ratio HR1 is defined as $(B-A)/(B+A)$, where A is the count rate between 0.1 and 0.4 keV and B is the count rate between 0.5 and 2.0 keV.

published photometry, (2) Guide Star Catalog (GSC) magnitudes, which suffer uncertainties of order 0.3 mag (Russell et al. 1990), or (3) our own flux-calibrated spectra. In case 2, visual magnitudes were derived from GSC "quasi B" magnitudes and $B-V$ colors. In case 3, we derived magnitudes and colors using the IRAF SBANDS routine to convolve our spectra with the U, B, and V transmission curves. Transparency variations and uncalibratable losses

TABLE 2

OBSERVATION LOG

UT (1996)	Name (EUVE)	t_{exp} (s)	Air Mass	Telescope
Jan 9:				
0828:34	J0831+402	300	1.01	2.4 m Hiltner
0857:05	J0736+257	3600	1.04	2.4 m Hiltner
Jan 10:				
0925:37	J0825−163	300	1.55	2.4 m Hiltner
0958:30	J1004+503	180	1.06	2.4 m Hiltner
1120:11	J1131−346	300	2.53	2.4 m Hiltner
Jan 11, 0643:40	J0609−358	300	2.68	2.4 m Hiltner
Jan 12:				
0149:48	J0009−105	1800	1.51	2.4 m Hiltner
0344:30	J0341−016	3600	1.20	2.4 m Hiltner
0916:32	J0702−018	1200	1.44	2.4 m Hiltner
0953:53	J0939+548	3600	1.09	2.4 m Hiltner
1110:43	J1031+508	1800	1.07	2.4 m Hiltner
1149:14	J1031+508	3600	1.09	2.4 m Hiltner
Jan 17, 0655:58	J0736+257	600	1.01	2.4 m Hiltner imaging
Apr 6, 1035:51	J1802+642	360	1.25	2.4 m Hiltner
Apr 9, 0718:27	J1256−032	600	1.22	2.4 m Hiltner
Apr 18:				
1249:00	J1145−553A	600	1.07	MSO 74 inch
1307:06	J1145−553B	300	1.09	MSO 74 inch
1657:20	J1713−858	600	1.57	MSO 74 inch
Apr 19, 0929:16.....	J0653−564	1800	1.18	MSO 74 inch
Apr 20:				
1523:06	J1535−774	2400	1.34	MSO 74 inch
1906:35	J2215−277	1200	1.34	MSO 74 inch
Apr 23:				
1621:29	J1811−789	600	1.41	MSO 74 inch
1735:49	J2110−193	300	1.51	MSO 74 inch
Apr 25:				
1927:44	J2244−332A	240	1.26	MSO 74 inch
1935:07	J2244−332B	240	1.24	MSO 74 inch

at the spectrograph slits make this procedure uncertain by up to ± 1 mag.

3. ANALYSIS

Our optical identifications are all based upon the discovery of members of known EUV-emitting classes through spectroscopy of objects within the combined *EUVE*/*ROSAT* error circles. We now discuss the new members of each of these classes in turn.

3.1. *The AGN Sample*

We have identified six extragalactic objects using optical spectroscopy: one BL Lac object, one Seyfert 2 galaxy, and four quasi-stellar objects (QSOs). Five of the identifications are previously unknown objects, and EUVE J1031+508 (=1ES 1028+511) was originally discovered in the *Einstein* Slew Survey (Elvis et al. 1992). All the AGNs detected are located within relatively low Galactic columns. With the exception of the BL Lac object (discussed below), all exhibit strong, narrow forbidden lines of oxygen, neon, and sulphur, as well as the hydrogen Balmer series. Spectra are presented in Figure 2.

Line widths were measured using the IRAF SPLOT routine to fit a Gaussian to a line. Measurements were then shifted to the rest frame and converted to velocity space. We derived redshifts from the forbidden lines only. Neutral hydrogen column densities were extracted from the Bell Laboratories H I Survey (Stark et al. 1992). Distances and absolute magnitudes were calculated assuming $H_0 = 50$ km s^{-1} Mpc^{-1}. Table 3 lists the positional, photometric (m_V, $B-V$, and *EUVE* and *ROSAT* count rates), and classification data. Table 3 also lists additional properties: H I column densities ($N_{\rm H}$), redshifts (z), distances (d), and absolute magnitudes (M_V). Table 4 lists velocity widths.

Our classifications are based upon the detections of nebulosity, the measured FWHM velocities of the permitted and forbidden emission lines according to the criteria of Osterbrock (1987), and absolute magnitudes. Osterbrock states that Seyfert 1 galaxies are characterized by $M_B \approx -21$, while for Seyfert 2 galaxies $M_B \approx -20$. However, a plot of absolute magnitude and object type (Weedman 1973) indicates some mixing between the two types, and therefore we discriminate between Seyfert 1 and Seyfert 2 galaxies based upon line widths. BL Lac objects tend to be more luminous than Seyfert galaxies. Weiler & Johnston (1980) cited a range from $M_V = -22$ to $M_V = -28$ for their sample of BL Lac objects. Schmidt & Green (1983) classified all objects with M_B fainter than -23 as Seyfert 1 galaxies. We have conducted imaging for only one object and thus have little evidence for their galactic nature. In addition, Seyfert 1 and QSO spectra are very similar. We therefore classify as QSOs objects with Seyfert 1/QSO spectra and no detected galaxy.

EUVE J0009−105, J0341−016, J0939+548, and J1256−032 all have permitted-line velocity widths in excess of 1000 km s^{-1}, characteristic of low-redshift quasars or Seyfert 1 galaxies.

We now present a brief overview of individual properties of the active galaxies.

EUVE J0009−105.—This object has been previously cataloged as PHL 2680, a blue-excess object. We now identify it as a QSO with redshift $z = 0.241$. The other, somewhat fainter, object just to the east of the error circle is a main-sequence G–K star, which is extremely faint and therefore an unlikely source of the EUV emission.

EUVE J0341−016.—The emission lines Hγ and [O III] λ4363 are blended together. We deblended the lines using the IRAF SPLOT routine, yielding an FWHM of 2100 km s^{-1} for Hγ. The prominent [O II] 3727 Å line has an FWHM of 700 km s^{-1}. These line widths lead us to a QSO classification.

EUVE J0736+257.—The Seyfert 2 galaxy EUVE J0736+257 has narrow permitted and forbidden lines of approximately the same width ($\approx$400 km s^{-1}). Characteristic of most Seyfert 2 galaxies, its emission lines exhibit blue-wing asymmetries (Weedman 1977; Khachikian & Weedman 1974). In addition, the Ca II H and K absorption lines of the host galaxy are seen quite clearly in the spectrum. We have detected nebulosity and elongation along a position angle of $\sim 45°$ in a red-band CCD image. Figure 3 compares the contour plots of the galaxy and of a stellar image taken from the same CCD frame.

EUVE J0939+548.—We classify EUVE J0939+548 as a low-redshift QSO based upon its emission lines and the lack of evidence for a host galaxy. This object has a redshift of $z = 0.292$ and an absolute magnitude of $M_V = -22.2$; it is somewhat more luminous than the typical Seyfert 1 galaxy, in accordance with its status as a QSO.

EUVE J1031+508.—The lone BL Lac object in our sample, EUVE J1031+508 (=1ES 1028+511) displays a high luminosity ($M_V = -25.1$) and nearly featureless continua, characteristic of most BL Lac objects. Previous studies of this object with the *Einstein* satellite have shown that, like many BL Lac objects, it is X-ray–bright (Elvis et al. 1992; Schachter et al. 1993) and exhibits a soft excess in the *ROSAT* PSPC bandpass (Bade, Fink, & Engels 1994). These studies also tentatively measured a redshift ($z = 0.239$) based upon optical spectroscopy and the uncertain detection of the Ca II H and K absorption lines (Perlman et al. 1996). None of the previously published spectra (Schachter et al. 1993; Perlman et al. 1996) exhibit the prominent Ca II H and K lines that we find, perhaps because of the lower quality of their spectra or the inherent variability of the object. Schachter et al. (1993) estimated 1–2 mag of variability between the POSS plate images and their 1993 spectroscopy. We have measured an accurate redshift of $z = 0.361$ based upon the prominent Ca II H and K lines present in our spectra. Bade et al. (1994) have studied EUVE J1031+508 and fitted a two-component power law, with neutral hydrogen column density as a free parameter, to its *ROSAT* PSPC spectra. They concluded that below 0.7 keV the slope was characterized by $\alpha = -2.4$, while above 0.7 keV $\alpha = -0.94$. The best-fit column density was $N_{\rm H} = 3.15 \times 10^{20}$, in sharp contrast to the 1.3×10^{20} measured by the Bell Laboratories survey. They postulated that the disagreement between the Bell Laboratories value and their best fit might be due to the presence of intrinsic absorption or the insufficiency of their fit model. This object has also been detected by many observers in the radio band at 6 cm (Becker, White, & Edwards 1991; Gregory & Condon 1991; Perlman et al. 1996). A spectral energy distribution comprising all known detections, and utilizing the Bade et al. (1994) fit, is presented in Figure 4.

EUVE J1256−032.—We identify EUVE J1256−032 as a low-redshift QSO, with $z = 0.318$, based upon its emission-line widths. This object also has $M_V \approx -23$, very near Schmidt & Green's (1983) faint limit for QSOs.

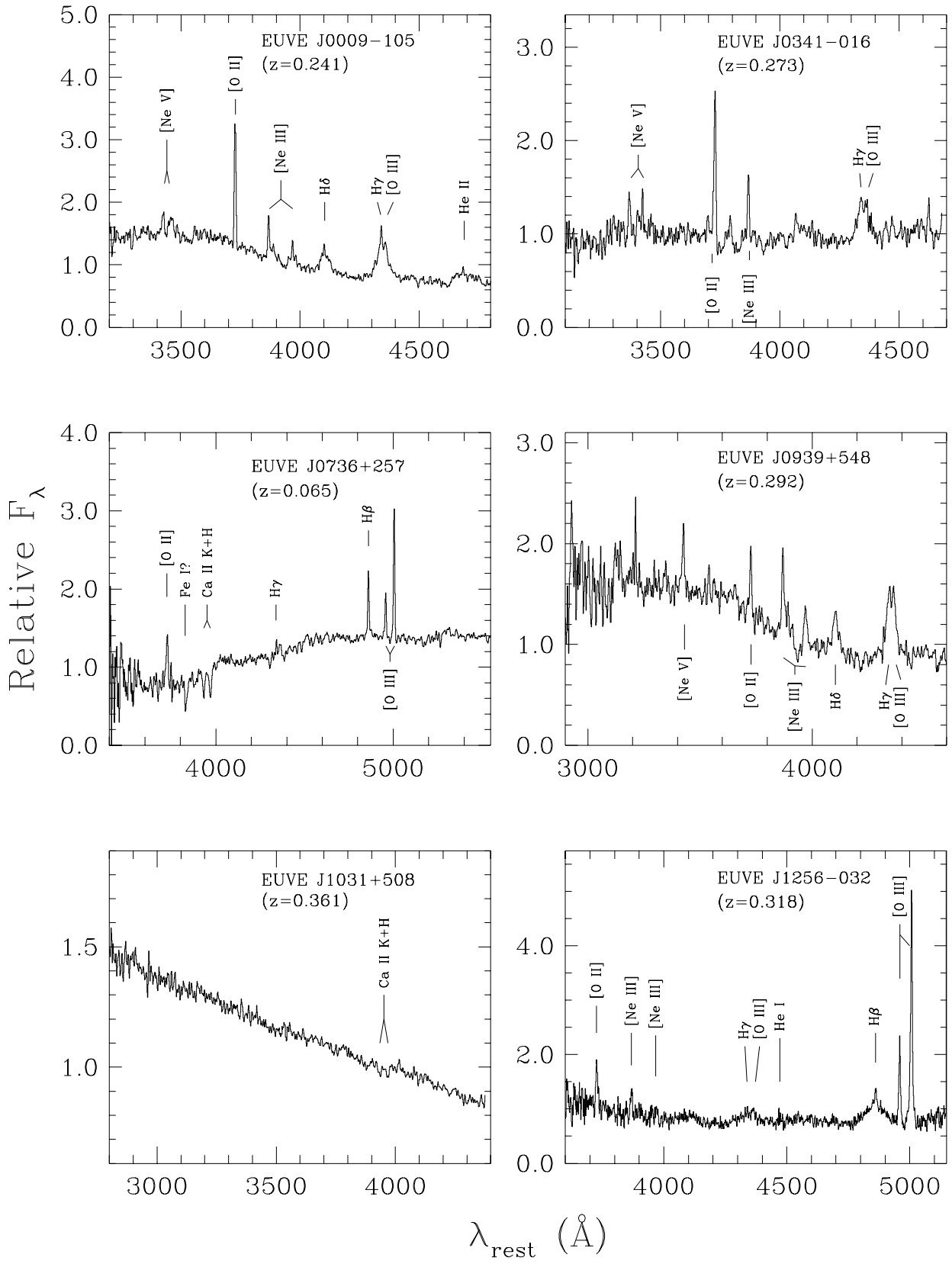

FIG. 2.—Optical spectra of the six AGNs: EUVE J0009−105, a QSO; EUVE J0341−016, a QSO; EUVE J0736+257, a Seyfert 2 galaxy; EUVE J0939+548, a QSO; EUVE J1031+508, a BL Lac object; and EUVE J1256−032, a QSO. The spectra have been smoothed by 3 pixels to reduce the noise levels and normalized to the flux at the 4000 Å rest wavelength.

TABLE 3

AGN SAMPLE

Name (EUVE)	R.A. (J2000)	Decl. (J2000)	m_V[a]	Spectral Type	$EUVE$[b] (counts s^{-1})	$ROSAT$[b] (counts s^{-1})	$B-V$	N_H (10^{20} cm^{-2})	z[c]	d[d] (Mpc)	M_V	Comments
J0009−105.....	00 09 04.5	−10 34 29.2	18.6[e]	QSO	0.045	0.07	0.11	3.08	0.241	1446	−22.2	PHL 2680
J0341−016.....	03 41 44.56	−01 41 42.23	19.52	QSO	0.032	0.02	0.63	7.41	0.273	1638	−21.6	
J0736+257.....	07 36 27.29	+25 44 11.82	17.29	Seyfert 2	0.036	0.07	1.01	5.39	0.065	390	−20.7	See Fig. 3 for imaging
J0939+548.....	09 39 31.83	+54 49 09.28	19.03	QSO	0.02	0.05	0.15	1.34	0.292	1752	−22.2	
J1031+508.....	10 31 18.47	+50 53 36.54	16.6[f]	BL Lac	0.02	4.66	0.35	1.15	0.361	2166	−25.1	1ES 1028+511
J1256−032.....	12 56 44.53	−03 14 46.52	18.79	QSO	0.022	0.07	...	1.70	0.318	1908	−22.6	No B magnitude

NOTE.—Units of right ascension are hours, minutes, and seconds, and units of declination are degrees, arcminutes, and arcseconds.

[a] Derived using the IRAF SBANDS utility unless otherwise noted.

[b] From Lampton et al. 1997.

[c] Derived from forbidden lines only.

[d] Assuming $H_0 = 50$ km s^{-1} Mpc^{-1}.

[e] From SIMBAD.

[f] Perlman et al. 1996.

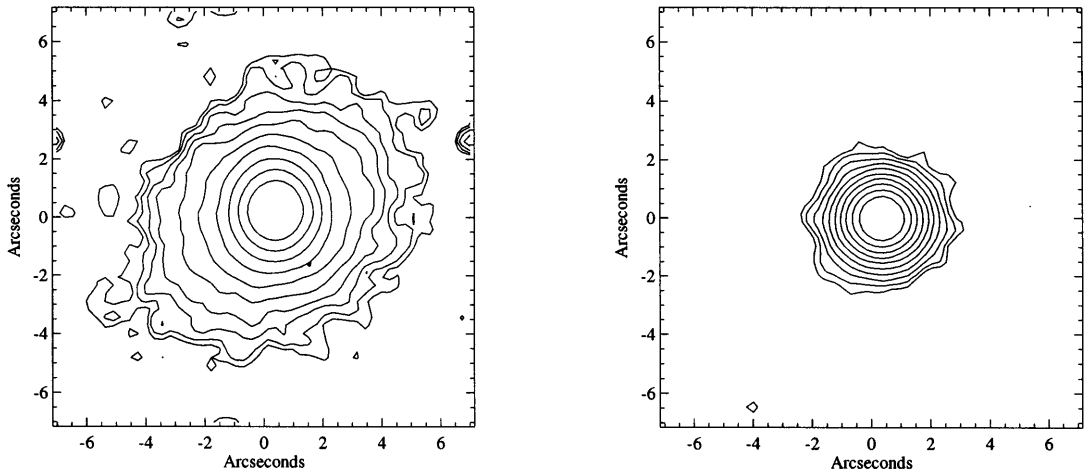

FIG. 3.—Contour plots of *R*-band images of EUVE J0736+257 (*left*) and a nearby star (*right*), taken from the same CCD frame. Minimum and maximum contour levels are 10 and 1000, respectively. Each contour increases by a factor of 1.67. The air mass was 1.010 at the start of the exposure and the seeing approximately 1".3. East is up and north is to the right. Note the extension to the northeast and southwest.

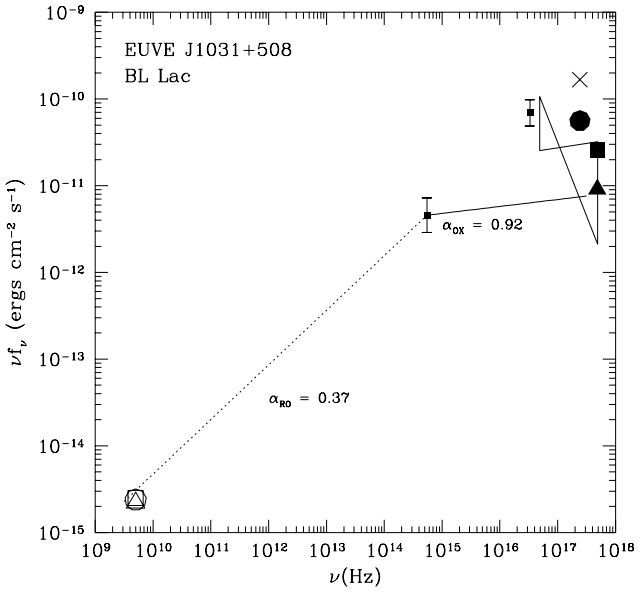

FIG. 4.—Energy spectrum of EUVE J1031+508. The 6 cm data shown are from Becker, White, & Edwards (1991; *open circle*), Gregory & Condon (1991; *open square*), and Perlman et al. (1996; *open triangle*). The X-ray bow-tie diagram and the optical and EUV data points are from this paper. *Einstein* Slew Survey data points are from Giommi, Ansari, & Micol (1995; *filled square*) and Perlman et al. (1996; *filled triangle*), and the *ROSAT* PSPC data points are from Nass et al. (1996; *filled circle*) and Bade, Fink, & Engels (1994; *cross*). The spectral indices are from Bade et al. (1994).

3.2. *The AGN Spectral Energy Distribution*

The X-ray slopes for AGNs depend upon the observed energy ranges. Several studies have shown that X-ray–selected samples of AGNs observed with the *Einstein* IPC (0.2–3.5 keV) have X-ray slopes between 0.25 and 1.5 (Wilkes & Elvis 1987; Elvis et al. 1994). Wilkes & Elvis (1987) present a histogram of their sample of 47 objects that spans this range but is dominated by objects with slopes between 0.3 and 1.3. The sample is double peaked; radio-loud objects cluster around $\alpha = 0.5$, and radio-quiet objects cluster around $\alpha = 1.0$. Work by Kruper, Urry, & Canizares (1990) confirms these results. For a sample of 75 Seyfert galaxies, they found that α ranges from approximately 0.2 to 1.3 and divides into $\alpha = 0.55$ for radio-loud objects and $\alpha = 0.80$ for radio-quiet objects.

The *ROSAT* PSPC has a slightly softer energy range (0.1–2.4 keV) than the IPC. Several recent studies indicate that the X-ray slope of AGNs is steeper in this energy range. Lieu et al. (1995) found $\alpha \approx 1.4$–2.3 for their sample of six AGNs. Walter & Fink (1993) studied a sample of 58 Seyfert 1 galaxies and found a slope of 1.3–2.7. Laor et al. (1994) fitted an X-ray slope ranging from 0.9 to 2.1 for their optically selected sample of 10 QSOs. Fiore et al. (1994) studied six radio-quiet QSOs and found a slope of 1.3–2.3. Some evidence also indicates that BL Lac objects may have a unique distribution of X-ray slopes. Brinkman et al. (1995) studied a sample of 59 radio detected BL Lac objects, for which they found an average slope of $\alpha = 1.28 \pm 0.58$. We

TABLE 4

VELOCITY WIDTHS OF FORBIDDEN AND PERMITTED LINES FOR AGNS

NAME (EUVE)	VELOCITY (km s^{-1})					
	[O II] λ3727	Hδ (4101 Å)	Hγ (4340 Å)	Hβ (4861 Å)	[O III] λ4959	[O III] λ5007
J0009−105.....	419	2723	...	...	...	...
J0341−016.....	695	...	2103	...	...	...
J0736+257.....	...	...	...	405	...	352
J0939+548.....	619	1710	...	...	...	...
J1256−032.....	...	...	...	5115	361	...

have chosen an X-ray slope of 0.9–2.7 for our *EUVE*/*ROSAT*-detected sample based upon the preceding factors. The fluxes are computed in the same fashion as in our study of the Seyfert 1 galaxy Ton S180 (Vennes et al. 1995).

We present spectral energy distributions spanning the optical to X-ray range in Figure 5. Our sample is X-ray–selected; the objects are faint optically but are significant *ROSAT* detections in the 0.1–2.4 keV range. Determining whether our objects are radio-quiet or radio-loud is difficult. No radio detections exist in the current literature, except for EUVE J1031+508. Wilkes & Elvis (1987) found a positive correlation between X-ray strength and radio strength. X-ray–bright objects should be radio-loud; if our objects could be classified as X-ray–bright, then the X-ray slopes would be more tightly constrained than we have indicated in Figure 5.

The EUV fluxes of these objects are of great astrophysical importance. The EUV flux of our sample is evident as an excess above the optical to X-ray continua. This excess could be a continuation of the optical/UV "blue bump" seen in many AGNs (Malkan & Sargent 1982). The "blue bump" feature may extend into the soft X-ray range in many objects, and has been modeled as the signature of an accretion disk surrounding a black hole that powers the AGNs (Malkan 1983; Elvis et al. 1994). The physical modeling of this spectral region is very controversial; some authors have proposed more complex scenarios than the widely accepted black hole–accretion disk model (Czerny & Życki 1994). If confirmed, the EUV detections have great implications for the nature of the "blue bump" and the engine of AGNs. We recommend long-duration *EUVE* exposures and *ROSAT* soft-band observations of this exceptional sample of EUV/X-ray–selected objects.

3.3. *The Active Dwarf Stars*

The active stars in our sample consist of a group of young, late-type K and M dwarfs with varying degrees of Ca II H and K emission. The optical, EUV, and X-ray fluxes of these stars originate in the chromosphere and corona, where the magnetic energy generated by the dynamo action is dissipated (Mathioudakis et al. 1995b).

The optical spectra are characterized by hydrogen Balmer line emission, as well as strong molecular absorption bands of TiO, CaOH, and MgH. The intensities of these absorption bands may be used to identify the spectral types because of their extreme sensitivity to temperature (Mathioudakis & Doyle 1991; Pettersen & Hawley 1989). The $B-V$ colors for these objects may be misleading if used for classification. Color indices for late-type stars have large values because of the steep slope of color as a function of temperature (Jaschek & Jaschek 1987). This slope results in large differences in $B-V$ colors if the mean wavelength of the photometric system is subject to any uncertainties. Thus, we did not attempt classification of the latest types utilizing the color indices but have noted below when they are discrepant with our spectral types. We present spectra of our 14 objects in Figure 6.

The late-type stars often exhibit flare activity (Pettersen 1989); flares have been detected in the EUV bandpass from AU Mic, EUVE J2056−171 (Mathioudakis et al. 1995a), and others. Stellar activity is linked to both the star's age and its spectral type; stronger flare activity correlates with

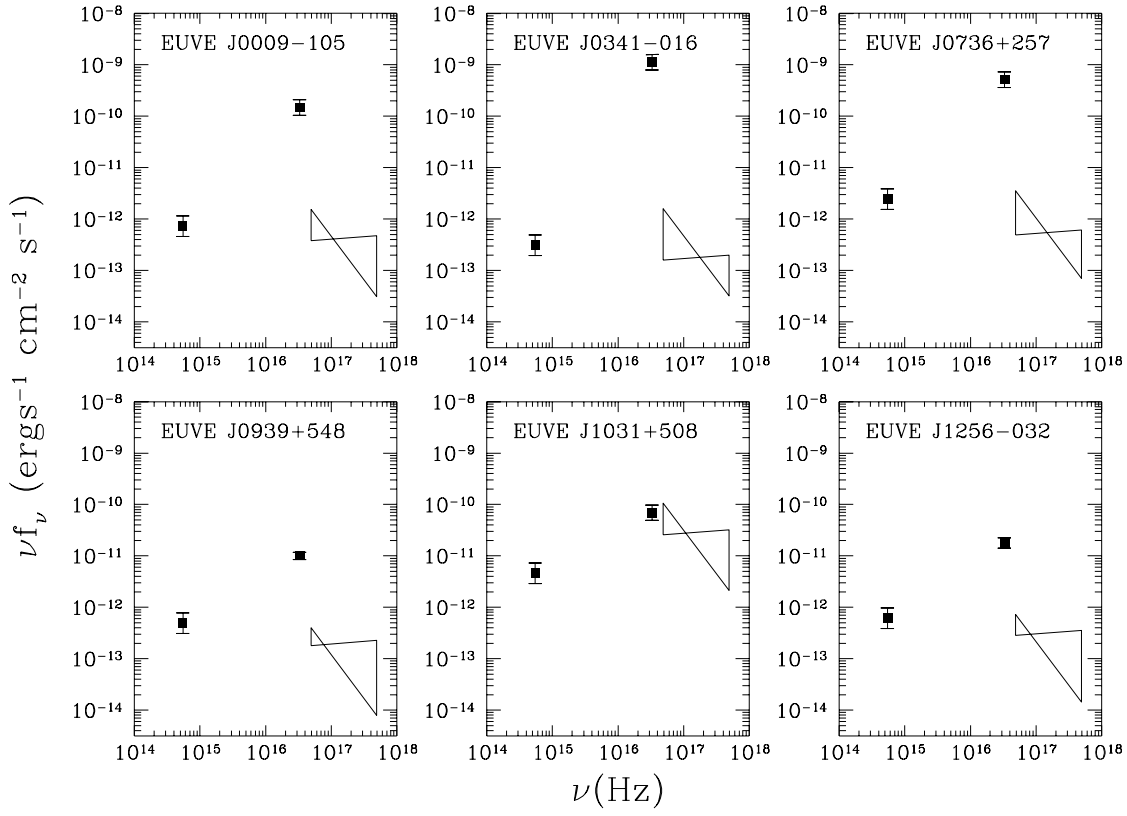

FIG. 5.—Observed optical to X-ray energy spectra of our sample of six AGNs. EUV and X-ray data are derived from the *EUVE* and *ROSAT* fluxes, and the EUV/X-ray slopes were chosen to range from 0.9 to 2.7 (see text).

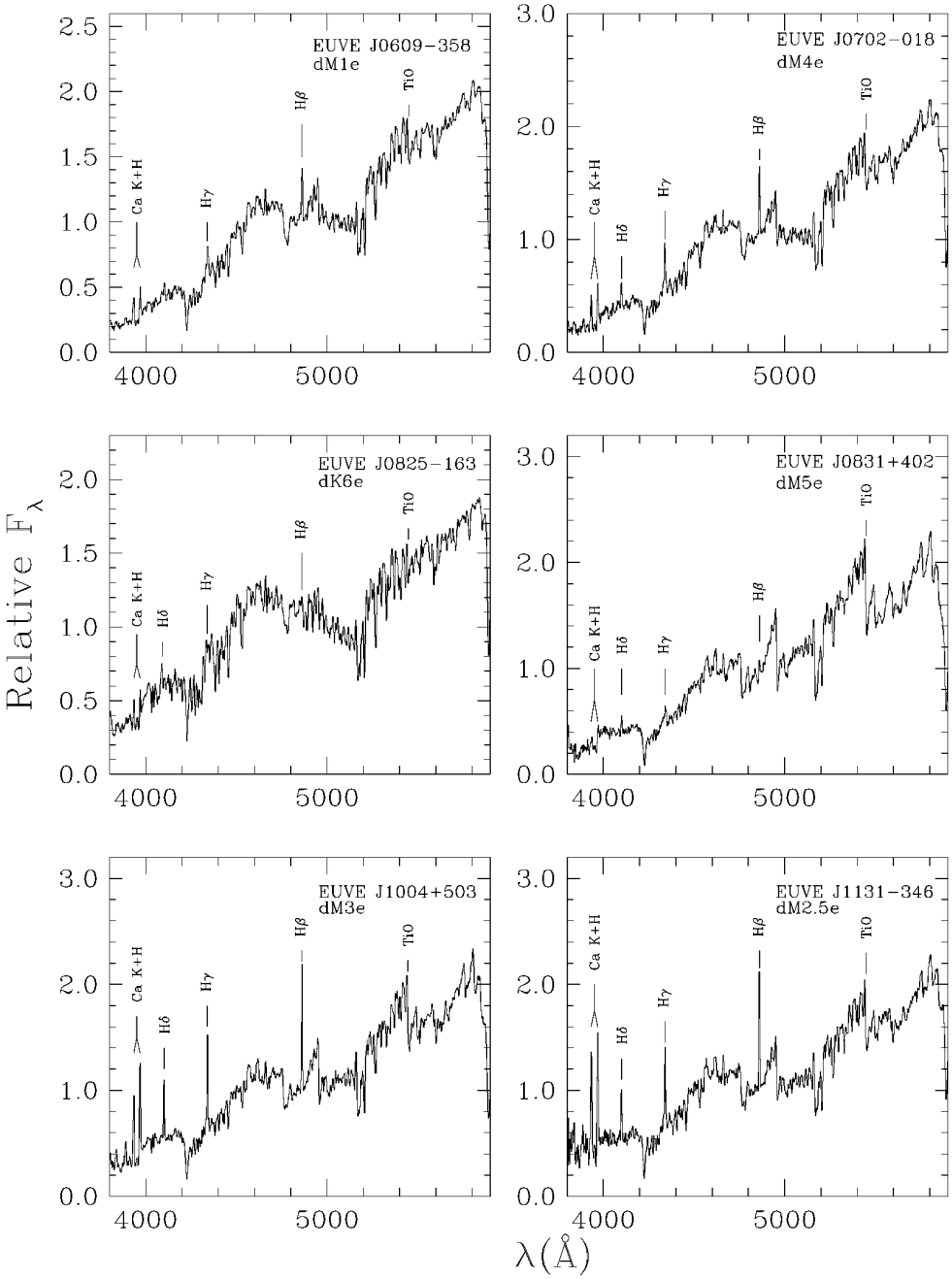

FIG. 6.—Optical spectra of the 14 active stars. The spectra have been normalized to the flux at 5000 Å.

later types and youth (Mathioudakis et al. 1995a; Linsky 1988). In great contrast with the Sun, for which optical flares are rare (Linsky 1988), late-type M dwarfs may exhibit as many as half a dozen optical flares per hour (Pettersen, Cochran, & Barker 1985). During a flare, the hydrogen emission lines become more pronounced and higher members of the series begin to appear (Linsky 1988; Foing 1989). X-ray emission may also be enhanced, and Ca II H and K may appear in emission. Pettersen & Hawley (1989) state that the strength of the Ca II and H I emission lines is a good indicator of the level of chromospheric activity.

We determined the absolute magnitudes of the active stars from the strength of the strongest TiO absorption bands using the criteria developed by Pettersen & Hawley (1989). TiO decrements were measured for the active stars using the IRAF SPLOT routine. Table 5 lists distances implied by the absolute and apparent magnitudes.

Spectral types for the M stars were derived based upon the luminosities, using Allen (1973), and by comparison with Pettersen & Hawley's (1989) spectra of flare stars. We estimate an uncertainty of one spectral type in our classifications, based upon the scatter in the Pettersen & Hawley (1989) relationship between absolute magnitude and the TiO decrement. Spectral types for the K stars, whose TiO bands are weaker, were inferred from the $B-V$ colors (Allen 1973).

EUV and X-ray fluxes were determined from the known

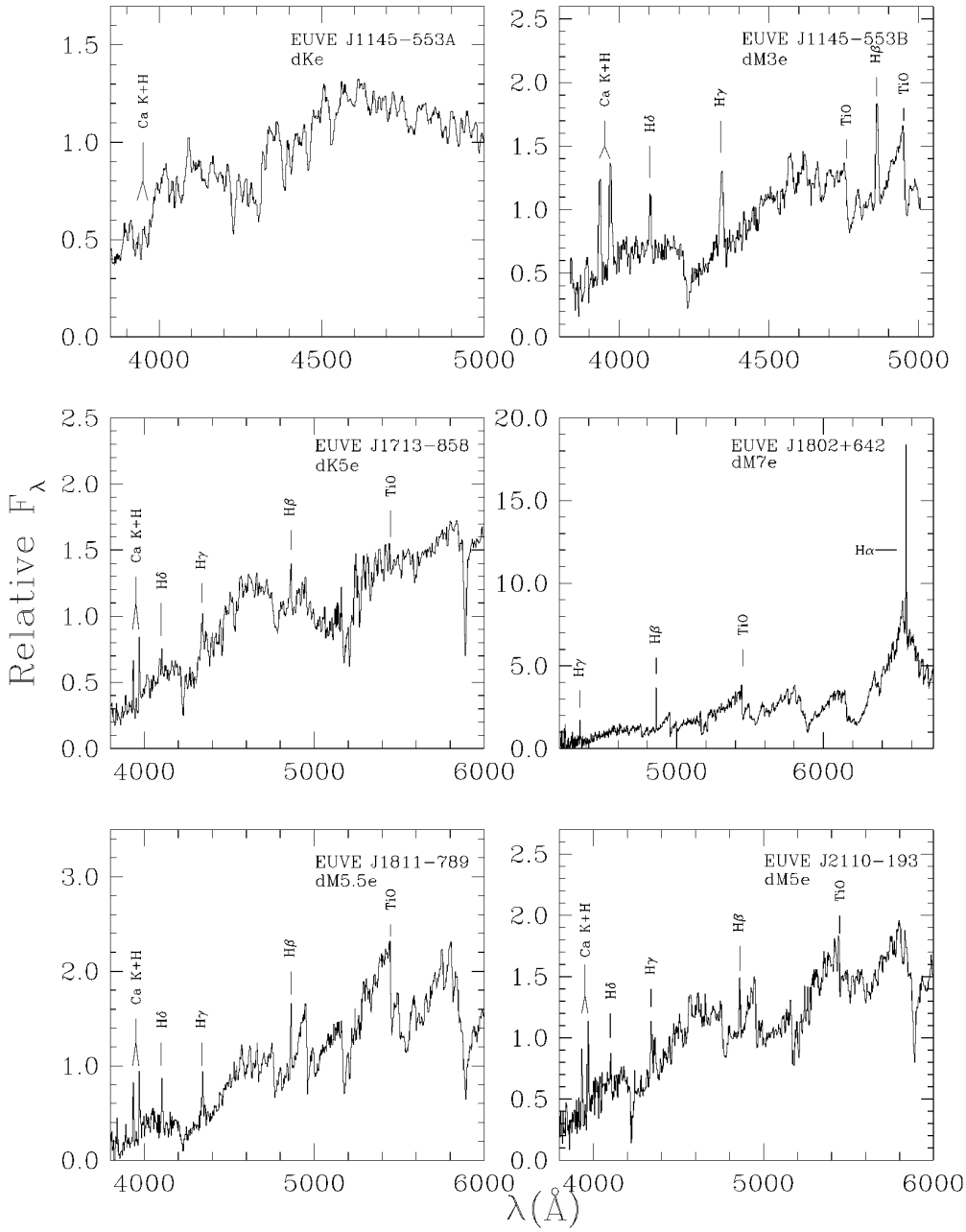

FIG. 6—*Continued*

count rates by estimating the hydrogen column density and assuming a coronal model (Monsignori-Fossi & Landini 1994). Since these stars are located nearby, we do not have any field objects in their direction that could be used to accurately estimate the hydrogen column densities. Hydrogen columns along the line of sight were estimated from the average interstellar medium (ISM) density (0.1 cm^{-3}; Cox & Reynolds 1987) and the distances. These data are presented in Table 5. The interstellar attenuation was computed using the compilation of hydrogen and helium photoionization cross sections presented by Rumph, Bowyer, & Vennes (1994). Source fluxes were determined using the Monsignori-Fossi & Landini (1994) line emissivities for a coronal temperature of 10^7 K. We believe this value is a good choice for the coronal temperature, as *EUVE* spectroscopic observations of the brightest dMe flare stars have shown that the Lexan/B band is dominated by lines of Fe XVIII–XXIII formed at around $10^{6.8}$–$10^{7.2}$ K. In order to evaluate an uncertainty for the estimated fluxes, we have examined their dependence upon the coronal temperature. At high interstellar hydrogen column densities, e.g., 1.5×10^{19} cm^{-2}, we find that a variation in the coronal temperature between 4×10^6 and 1.5×10^7 K results in a maximum change of 30% in the Lexan/B flux. For the same coronal temperature, 10^7 K, a change in the hydrogen column density from 1.5×10^{19} to 5×10^{18} cm^{-2} causes a 50% change in the flux. The small influence of N_H on the *ROSAT* PSPC wavelengths makes the uncertainty of the fluxes considerably smaller. We calculated surface fluxes based upon the method outlined in Oranje, Zwaan, & Mid-

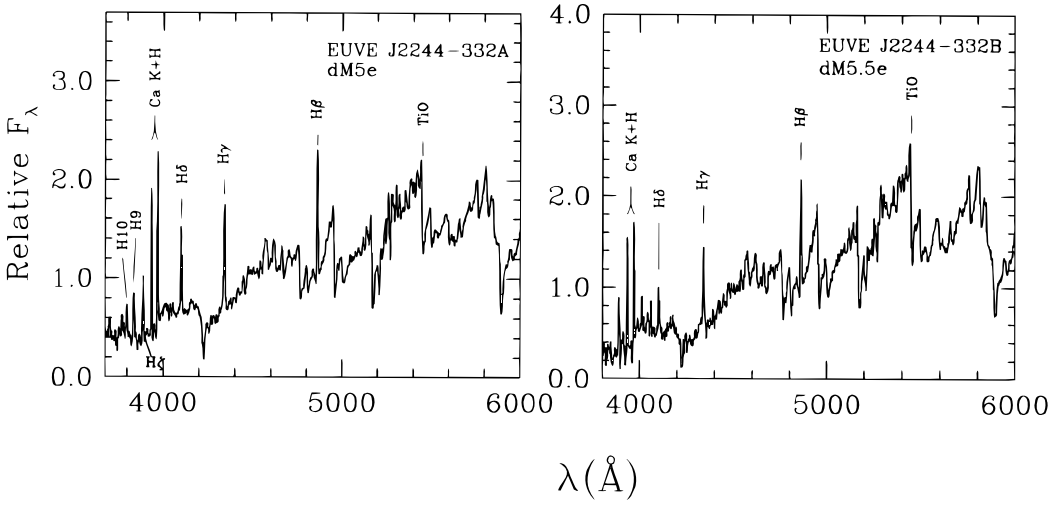

FIG. 6—*Continued*

dlekoop (1982). Bolometric corrections and effective temperatures for the M and K stars were based upon the spectral types and interpolated from Allen's (1973) tables. Table 6 lists the *EUVE* and *ROSAT* PSPC fluxes.

We now present a brief overview of individual properties of the active stars.

EUVE J0609−358.—The spectral type of EUVE J0609−358 is uncertain. This object has a $B-V$ color indicative of an M2 V star, and its spectrum is most similar to an M1 V star, as depicted by Pettersen & Hawley (1989). However, criteria based upon TiO bands disagree on absolute luminosities; the TiO 4950 and 5450 Å bands provide $M_V = 7.8$, characteristic of dK6.5 stars, and the weaker TiO 4760 Å band yields $M_V = 9.44$, which would place this object in the M1 V class, in agreement with its spectral shape. The overluminous nature of this object is puzzling.

EUVE J0702−018.—This object is located in a dense field. We conducted spectroscopy of all the stars within the error circle; they were all inactive K–G types. We identify EUVE J0702−018 as a dM4e star.

EUVE J0825−163.—The star EUVE J0825−163 is identified in the second *ROSAT* Wide Field Camera (WFC) source catalog (2RE; Pye et al. 1995) as GSC 5998-1783. We identify the EUV source with the star GSC 5998-1918 and assign a dK6e spectral type. Because of the large error circles of the WFC and *EUVE*, the 2RE identification may be a second source. Optical spectra would be necessary to confirm the second source.

EUVE J0831+402.—This object is also known as GSC 2978-1686. The GSC lists the quasi-V magnitude as 13.32. We derive a spectral type of dM5e.

EUVE J1004+503.—We identify the star EUVE J1004+503 as the previously known, high proper motion Giclas object G196-3 (Giclas, Burnham, & Thomas 1966). We classify this star as dM3e.

EUVE J1131−346.—EUVE J1131−346 (PDS 55, or CD −33°7795) is also known from the Pico dos Dias survey for T Tauri stars. Gregorio-Hetem et al. (1992) classified PDS 55 as an isolated T Tauri star associated with the TW Hya group, based upon its proximity to TW Hya and

TABLE 5

ACTIVE STAR SAMPLE

Name (EUVE)	m_V	Spectral Type	$B-V$	M_V (TiO 5450 Å)	d (pc)	N_H (10^{18} cm^{-2})	Comments
J0609−358.....	11.05	dM1e	1.52	7.8	45	<13.9	GSC 7084-0794
J0702−018.....	13.46–14.51[a]	dM4e	1.58	9.15	73–118	22.5–36.4	No GSC magnitude
J0825−163.....	10.52	dK6e	1.22	7.2	46	<14.2	GSC 5998-1918
J0831+402.....	13.32[b]	dM5e	1.67	11.8	20	<6.2	GSC 2978-1686
J1004+503.....	11.29[b]	dM3e	1.44	10.5	14	<4.3	GSC 3440-0013
J1131−346.....	11.54	dM2.5e	1.4	10.3	18	<5.6	GSC 7223-0275
J1145−553B.....	13.86 (m_B)[c]	dM3e	1.55[d]	10.6 (4950 Å)	22[e]	<6.8	3850–5000 Å only
J1713−858.....	11.69	dK5e	1.21	7.0	87	<26.8	GSC 9526-0895
J1802+642.....	12.92	dM7e	2.68[f]	14.5	5	<1.5	GSC 4209-1465
J1811−789.....	12.38	dM5.5e	1.7	12.7	9	<2.8	GSC 9453-1008
J2110−193.....	11.75	dM5e	1.25	9.5	28	<8.6	GSC 6354-0357
J2244−332A.....	12.05	dM5e	1.28	12.25	9	<2.8	GSC 7501-0987
J2244−332B.....	13.29	dM5.5e	1.47	13.7	8	<2.5	GSC 7501-0943

[a] Range estimated from other stars on GSC plate and spectrophotometry.
[b] From the GSC.
[c] SBANDS B magnitude.
[d] Estimated from spectral type.
[e] Distance estimated using distance modulus and m_V estimated from spectral type.
[f] $B-V$ derived from uncertain B-value in SIMBAD; our spectra only 4200–6800 Å.

TABLE 6

EUVE/ROSAT Count Rates and Fluxes for Active Stars

Name (EUVE)	R.A. (J2000)	Decl. (J2000)	*EUVE* Count Rate (counts s^{-1})	*EUVE* Flux (10^{-13} ergs cm^{-2} s^{-1})	*ROSAT* Count Rate (counts s^{-1})	*ROSAT* Flux (10^{-13} ergs cm^{-2} s^{-1})
J0609−358.....	06 09 19.13	−35 49 30.0	0.019	12	0.42	30
J0702−018.....	07 02 58.88	−01 48 40.62	0.030	30	0.02	1.5
J0825−163.....	08 25 51.81	−16 22 47.6	0.026	16	0.52	38
J0831+402.....	08 31 01.91	+40 12 13.76	0.024	9.5	0.13	9.0
J1004+503.....	10 04 21.68	+50 23 16.89	0.020	7.0	0.70	48
J1131−346.....	11 31 55.39	−34 36 27.3	0.022	8.5	0.70	48
J1145−553B.....	11 45 47.89	−55 20 30.1	0.018	7.5	0.51	35
J1713−858.....	17 13 08.5	−85 52 08.9	0.019	22	0.18	14
J1802+642.....	18 02 16.09	+64 15 51.16	0.007	2.1	0.17	11
J1811−789.....	18 11 14.67	−78 59 29.3	0.019	6.5	0.46	31
J2110−193.....	21 10 05.31	−19 19 55.5	0.027	14	0.37	26
J2244−332A.....	22 44 57.65	−33 14 59.3	0.036	12	0.89	60
J2244−332B.....	22 44 59.75	−33 15 23.7	0.036	12	0.89	60

Note.—Units of right ascension are hours, minutes, and seconds, and units of declination are degrees, arcminutes, and arcseconds.

the detection of strong Li I λ6708 absorption and Hα emission. Unlike many T Tauri stars, it was not detected by *IRAS*, and Jensen, Mathieu, & Fuller (1996) cite only an upper limit of 126 mJy for its 800 μm flux. It has also been detected in radio surveys at the VLA. Rucinski & Lim (1994) reported flux densities of 4.10 and 4.33 mJy at 6 and 3.6 cm, respectively. These authors also estimated the spectral type as M2 V–M3 V, in excellent agreement with our classification of M2.5 Ve. Although several authors have classified this object as a T Tauri or weak-lined T Tauri (WTT) star based upon the strength of its Hα and Li I lines, its classification remains in doubt. Mathioudakis et al. (1995a) have studied a similar object, the dK7e–dM0e star EUVE J2056−171, and have argued that the Li abundance could be produced during energetic flare events. In addition, Rucinski & Lim (1994) detected 10%–15% polarization at the VLA wavelengths, which is far in excess of that measured for known WTT stars (1%–2%; White, Pallavicini, & Kundu 1992). If EUVE J1131−346 is indeed a T Tauri star, it would be one of very few ever detected by *EUVE*. Additional study of this object with the *Hubble Space Telescope* and *EUVE* may clarify its nature.

EUVE J1145−553A,B.—EUVE J1145−553B is classified as a dM3e star. This object was also detected in the *Einstein* Slew Survey (1ES 1143−55.0), where it is listed as an unidentified source (Elvis et al. 1992). This object is located somewhat outside of the position error circle. A second source exists on the edge of the error circle. The K star EUVE J1145−553A has weak Ca II H and K emission. However, we believe that EUVE J1145−553B is a more likely candidate for the EUV detection, based upon its much stronger emission lines.

EUVE J1713−858.—Also known as GSC 9526-0895, this object has a quasi-*B* magnitude of 12.56 and a derived spectral type of dK5e.

EUVE J1802+642.—This star was originally detected in the Giclas, Burnham, & Thomas (1968) and the Luyten (1971) proper-motion surveys, where it is known as G227-22 and LP 71-82, respectively. We propose a dM7e spectral type. We note the possible variability of this object; Giclas et al. list a photographic magnitude of 14.8, Luyten lists a photographic magnitude of 15.5, and we derive a *V* magnitude of 12.92. This object has also been detected as an X-ray source in the *Einstein* IPC 2E survey as 2E 1802.0+6415 (McDowell 1994).

EUVE J1811−789.—This object is listed as GSC 9453-1008 with a quasi-*B* magnitude of 13.6. We derive a spectral type of dM5.5e.

EUVE J2110−193.—This object is listed as GSC 6354-0357 with a quasi-*B* magnitude of 12.65. We derive a spectral type of dM5e.

EUVE J2244−332A,B.—EUVE J2244−332B (TX PsA) is a well-known, nearby flare star originally detected in the Gliese (1969) and Luyten (1957) proper-motion surveys, where it is known as GJ 871.1B and LTT 9175 (or L574-61), respectively. This star is the secondary component of a common proper motion binary system comprising GJ 871.1B and GJ 871.1A (or LTT 9174, L574-62). Kunkel (1972) reported detection of a flare on the B component and listed the star's apparent visual magnitude as 12.5. Petit (1980) lists this star as a nearby variable. He derived a parallax of 0.060 and a spectral type of dM4e, close to our type of dM5.5e. Rodonó (1978) lists spectral types in the Joy & Abt (1974) scale for both members of the system, dM3e and dM4e for A and B, respectively, and cites their magnitudes as 13.0 and 14.4. Finally, Petit (1990) again lists GJ 871.1B as a flare star and measures its variability in the *U* band to be 15.2–16.6. We detect evidence for flare activity in the dM5e star EUVE J2244−332A. In this object, emission lines of Hζ and Hη appear prominently, as well as shorter wavelength members of the Balmer series down to H12. Interestingly, the emission reversal of the Ca I λ4227 absorption feature, which is a strong indicator of high activity, is lacking in this object (Mathioudakis & Doyle 1991).

Finally, in Figure 7, we plot the EUV surface fluxes as a function of the *ROSAT* surface fluxes. According to Mathioudakis et al. (1995b), the EUV radiative losses should be comparable to the X-ray losses. In fact, we do see a good correlation between the two fluxes. One star appears to deviate from the linear grouping: EUVE J0831+402 appears to have an unusually low X-ray flux. We postulate that this star may have been undergoing flare activity during the *EUVE* observations, thereby raising its EUV flux to higher than normal levels. The *ROSAT* observations may have been taken during a quiescent state.

3.4. *The White Dwarf Stars*

Young white dwarf stars, with temperatures in excess of 25,000 K, constitute a relatively large fraction of the membership in EUV survey catalogs (see Pye et al. 1995; Bowyer

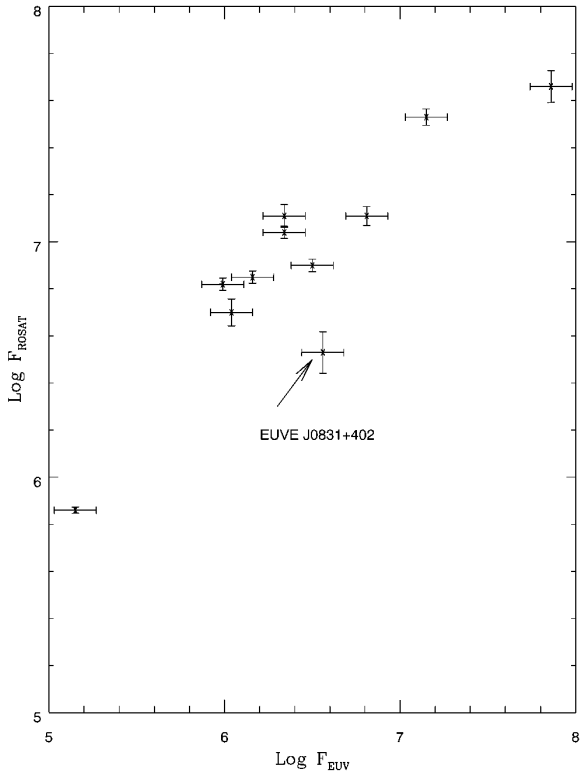

FIG. 7.—*EUVE* (0.05–0.2 keV) surface fluxes vs. *ROSAT* PSPC (0.1–2.4 keV) surface fluxes for 13 of the active stars (see Tables 5 and 6 and § 3.3). The *ROSAT* error bars were derived from the errors in the count rates as listed in Voges et al. (1997). The *EUVE* error bars were estimated at ±33% of the flux (a minimum 3 σ detection).

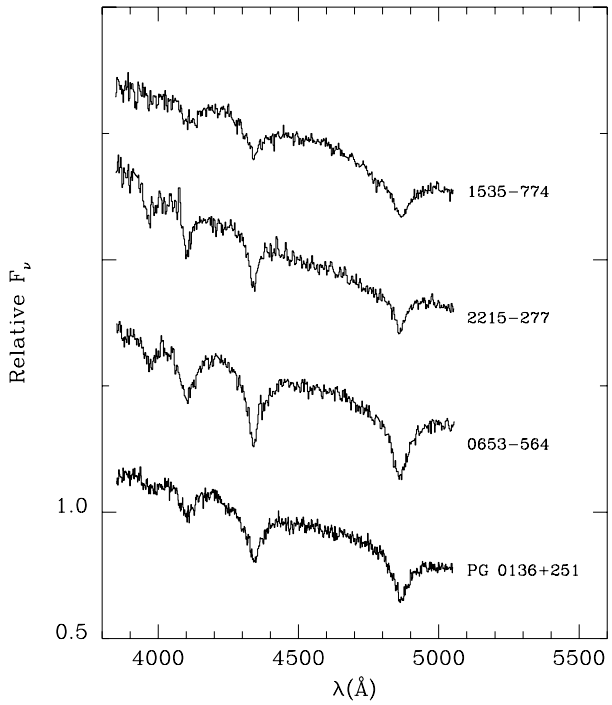

FIG. 8.—Optical spectra of three new white dwarf stars, the massive DA1 EUVE J0653−564 and DA0 EUVE J1535−774, and the DA0 EUVE J2215−277. A spectrum of the massive DA1 white dwarf PG 0136+251 (Schmidt et al. 1992) is shown for comparison.

et al. 1996; Lampton et al. 1997). The EUV-selected white dwarfs are often nearby ($d \approx 100$ pc; see Vennes et al. 1996b) and are most often the brightest EUV sources in the sky; a number of white dwarfs should, therefore, turn up in the optical identification of new EUV sources. These efforts may be hampered somewhat by the relative faintness in the optical range and low spatial density of these compact objects, as we show with three following cases. Study of the fields surrounding EUVE J0653−564, J1535−774, and J2215−277 reveals three new white dwarf stars (see Fig. 8 and Table 7). All three objects have estimated $V > 16$, and an analysis of their properties is most revealing.

Using optical spectroscopy, we determine the effective temperature and surface gravity of the three white dwarfs following the method described in Vennes et al. (1996b). Balmer line profiles in a hot, hydrogen-rich DA white dwarf depend upon the effective temperature and surface gravity of the star, which solely determine its atmospheric temperature and density structure. We computed a grid of hydrogen line-blanketed model atmospheres in local thermodynamic equilibrium and detailed model line profiles using the results of T. Schöning & K. Butler (1995, private communication). Figure 9 shows the results of line profile fits as a function of effective temperature ($T_{\rm eff}$) and the logarithm of the surface gravity (log g). Table 8 summarizes the stellar properties: $T_{\rm eff}$ and log g determined previously, the mass (M) in solar units determined from theoretical mass-radius relations (sequences with thin hydrogen layers from Wood 1995), the absolute V magnitude (M_V) determined from the model flux at 5500 Å, and finally the distance (d) measured from the $m_V - M_V$ distance modulus. Table 8 also compares the new white dwarfs with a known massive white dwarf (PG 0136+251; Schmidt et al. 1992) and the hot white dwarf HZ 43 (see Napiwotzki et al. 1993).

EUVE J0653−564.—Interestingly, EUVE J0653−564 is found to be a new massive white dwarf, with a mass well in excess of 1.1 $M_\odot$. The star is similar in temperature and surface gravity to PG 0136+251 (Schmidt et al. 1992). This object is classified as a DA1 in the system of Sion et al. (1983).

EUVE J1535−774.—This DA0 white dwarf is also a new massive white dwarf, but much hotter than most other objects of its category. It is also presumably much younger

TABLE 7

WHITE DWARF SAMPLE

Name (EUVE)	R.A. (J2000)	Decl. (J2000)	l (deg)	b (deg)	m_V	Spectral Type	*EUVE* (counts s^{-1})	*ROSAT* (counts s^{-1})
J0653−564.....	06 53 53	−56 24 44	266.3	−22.0	16.40	DA	0.012	0.07
J1535−774.....	15 35 45	−77 24 37	311.6	−17.4	16.46	DA	0.064	0.58
J2215−277.....	22 15 15	−27 42 18	22.7	−55.5	16.26	DA	0.028	0.35

NOTE.—Units of right ascension are hours, minutes, and seconds, and units of declination are degrees, arcminutes, and arcseconds.

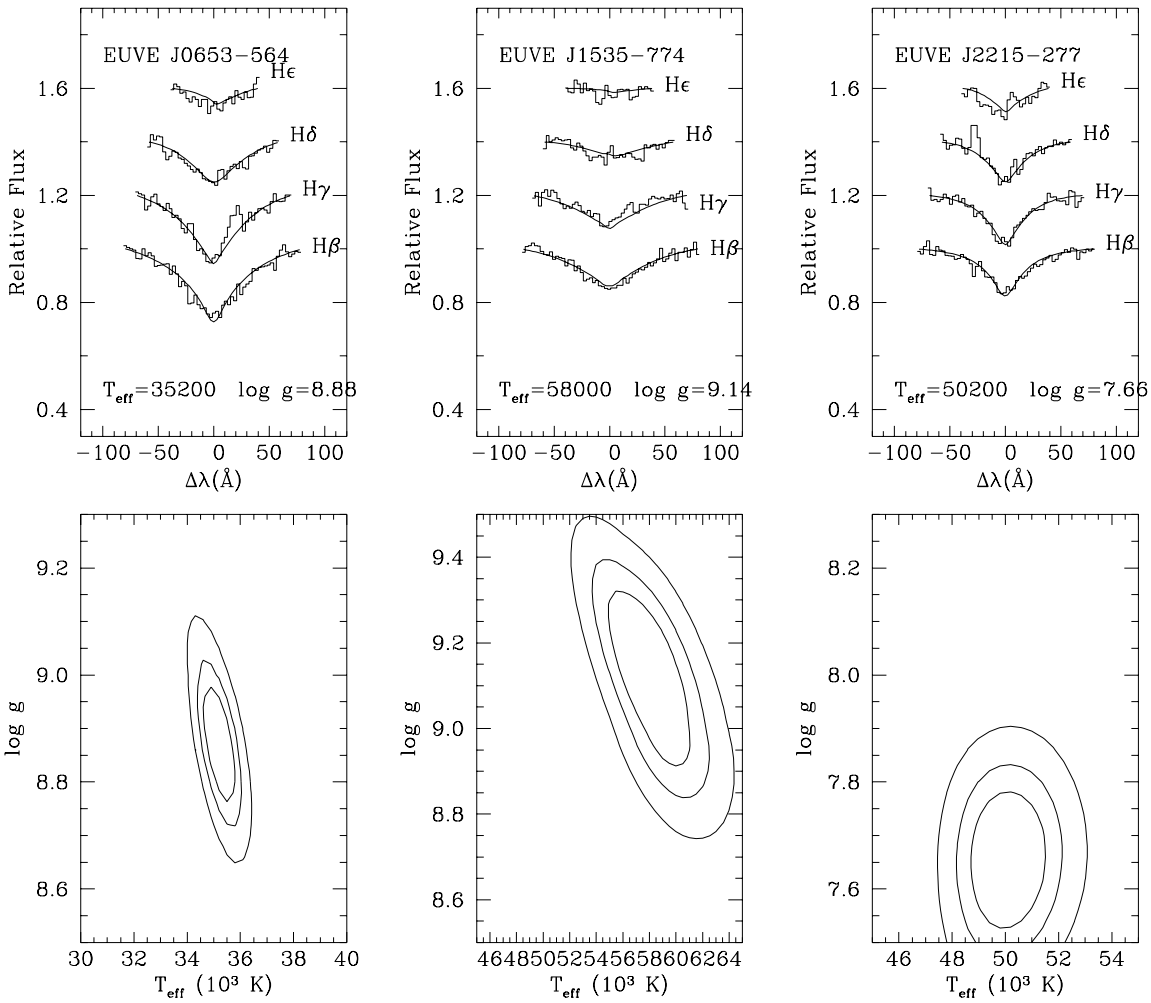

FIG. 9.—Fits to the Balmer line profiles of the new white dwarfs as a function of effective temperature ($T_{\rm eff}$) and surface gravity (log g) (*top*), and the 66%, 90%, and 99% confidence contours (*bottom*).

and could be a predecessor of the massive DA1 white dwarf GD 50. Vennes, Bowyer, & Dupuis (1996a) measured a relatively large photospheric abundance of helium in GD 50. The provenance of helium in a massive white dwarf remains unknown, and a study of the atmospheric composition of a younger object such as EUVE J1535−774 may help solve the question of the peculiar helium abundance and the mystery of the origin of massive white dwarfs.

EUVE J2215−277.—This DA1 white dwarf appears similar to the hot white dwarf HZ 43, but at a distance of 324 pc. Further studies of this object should aim at a determination of its atmospheric composition and the hydrogen column density in the ISM. The detection at EUV wavelengths of a white dwarf star implies a low density of hydrogen in this particular line of sight in the ISM.

These objects are either nearby but intrinsically faint because of their high surface gravity or, as in the case of EUVE J2215−277, intrinsically luminous but very distant. The discovery of two new massive white dwarfs in the solar neighborhood adds to Vennes et al.'s (1996b) proposition that a large population of massive white dwarfs may lie hidden in the solar vicinity. EUV surveys are naturally efficient in uncovering these peculiar objects.

4. SUMMARY

We have presented identifications of 21 new EUV sources. Sixteen of these sources are previously unknown objects. The other five (including two double stars) are present in a wide variety of catalogs. Our sample includes five unusual objects: a BL Lac object, for which we measure

TABLE 8

WHITE DWARF STELLAR PROPERTIES

Name	$T_{\rm eff}$ (K)	$\Delta T_{\rm eff}$ (K)	log g	Δ log g	M ($M_\odot$)	ΔM ($M_\odot$)	M_V	d (pc)
EUVE J0653−564.....	35,200	1250	8.88	0.22	1.14	0.06	11.26	107
EUVE J1535−774.....	58,000	6000	9.14	0.42	1.30	0.11	11.25	110
EUVE J2215−277.....	50,200	3580	7.66	0.25	0.50	0.05	8.71	324
PG 0136+251	39,190	360	9.00	0.10	1.21	0.05	11.35	85
HZ 43	49,000	2000	7.70	0.20	0.51	0.08	8.81	67

the first accurate redshift, a possible T Tauri star, which is the first such object ever detected in the EUV, a flare star with an unusually high level of activity, and two massive white dwarf stars. This ensemble of objects characterizes well the wide variety of sources observable with *EUVE*. Opportunities for additional discoveries may yet lie within the pool of detections in the *EUVE* survey.

The authors would like to express their thanks to Bob Barr at MDM and Mike Bessell at MSO for their help during the observing runs. This work was supported by NASA grant NAG 5-2636 and by a grant from the Sigma Xi Scientific Research Society. The Digitized Sky Surveys were produced at the Space Telescope Science Institute under US government grant NAGW-2166. The images of these surveys are based on photographic data obtained using the Oschin Schmidt Telescope on Palomar Mountain and the UK Schmidt Telescope. The plates were processed into the present compressed digital form with the permission of these institutions.

REFERENCES

Allen, C. W. 1973, Astrophysical Quantities (3d ed.; London: Athlone)
Bade, N., Fink, H. H., & Engels, D. 1994, A&A, 286, 381
Becker, R. H., White R. L., & Edwards, A. L. 1991, ApJS, 75, 1
Bowyer, S., Lampton, M., Lewis, J., Wu, X., Jelinsky, P., & Malina, R. F. 1996, ApJS, 102, 129
Brinkman, W., Siebert, J., Reich, W., Fürst, E., Reich, P., Voges, W., Trümper, J., & Wielebinski, R. 1995, A&AS, 109, 147
Cox, D. P., & Reynolds, R. J. 1987, ARA&A, 25, 303
Czerny, B., & Życki, P. T. 1994, ApJ, 431, L5
Elvis, M., Plummer, D., Schachter, J., & Fabbiano, G. 1992, ApJS, 80, 257
Elvis, M., et al. 1994, ApJ, 95, 1
Fiore, F., Elvis, M., McDowell, J. C., Siemiginowska, A., & Wilkes, B. J. 1994, ApJ, 431, 515
Foing, B. 1989, in IAU Colloq. 104, Solar and Stellar Flares, ed. B. M. Haisch & M. Rodonó (Dordrecht: Kluwer), 117
Giclas, H. L., Burnham, R., & Thomas, N. G. 1966, Lowell Obs. Bull., 6, 271
———. 1968, Lowell Obs. Bull., 7, 67
Giommi, P., Ansari, S. G., & Micol, A. 1995, A&AS, 109, 267
Gliese, W. 1969, Catalogue of Nearby Stars (Veröff. Astron. Rechen-Inst. Heidelberg, No. 22) (Karlsruhe: G. Braun)
Gregorio-Hetem, J., Lépine, J. R. D., Quast, G. R., Torres, C. A. O., & de la Reza, R. 1992, AJ, 103, 549
Gregory, P. L., & Condon, J. J. 1991, ApJS, 75, 1011
Jaschek, C., & Jaschek, M. 1987, The Classification of Stars (Cambridge: Cambridge Univ. Press)
Jensen, E. L. N., Mathieu, R. D., & Fuller, G. A. 1996, ApJ, 458, 312
Joy, A. H., & Abt, H. A. 1974, ApJS, 28, 1
Khachikian, E. Y., & Weedman, D. W. 1974, ApJ, 192, 581
Kruper, J. S., Urry, C. M., & Canizares, C. R. 1990, ApJS, 74, 347
Kunkel, W. E. 1972, Inf. Bull. Variable Stars, No. 748
Lampton, M., Lieu, R., Schmitt, J. H. M. M., Bowyer, S., Voges, W., Lewis, J., & Wu, X. 1997, ApJS, 108, 545
Lampton, M., Margon, B., Paresce, F., Stern, R., & Bowyer, S. 1976, ApJ, 203, L71
Laor, A., Fiore, F., Elvis, M., Wilkes, B. J., & McDowell, J. C. 1994, ApJ, 435, 611
Lieu, R., Mittaz, J., Bowyer, S., Lewis, J., & Hwang, C.-Y. 1995, Adv. Space Res., 16(3), 81
Linsky, J. L. 1988, in Multiwavelength Astrophysics, ed. F. A. Córdova (Cambridge: Cambridge Univ. Press)
Luyten, W. J. 1957, A Catalogue of 9867 Stars in the Southern Hemisphere with Proper Motions Exceeding 0".2 Annually (Minneapolis: Lund Press)
———. 1971, Proper Motion Survey with the 48 Inch Schmidt Telescope: The Zones +66° and +60°, 6^h to 20^h (Minneapolis: Univ. Minnesota)
Malkan, M. A. 1983, ApJ, 268, 582
Malkan, M. A., & Sargent, W. L. W. 1982, ApJ, 254, 22
Mathioudakis, M., & Doyle, J. G. 1991, A&A, 244, 409
Mathioudakis, M., et al. 1995a, A&A, 302, 422
Mathioudakis, M., Fruscione, A., Drake, J. J., McDonald, K., Bowyer, S., & Malina, R. 1995b, A&A, 300, 775
McDowell, J. C. 1994, *Einstein Observatory* Unscreened IPC Data Archive (SAO High-Energy Astrophys. Div. CD-ROM Ser. 1, Nos. 18–36) (Cambridge: Smithsonian Astrophys. Obs.)
Monsignori-Fossi, B., & Landini, M. 1994, Sol. Phys., 152, 81
Napiwotzki, R., Barstow, M. A., Fleming, T., Holweger, H., Jordan, S., & Werner, K. 1993, A&A, 278, 478
Nass, P., Bade, N., Kollgaard, R. I., Laurent-Muehleisen, S. A., Reimers, D., & Voges, W. 1996, A&A, 309, 419
Oranje, B. J., Zwaan, C., & Middlekoop, F. 1982, A&A, 110, 30
Osterbrock, D. E. 1987, Astrophysics of Gaseous Nebulae and Active Galactic Nuclei (Mill Valley, CA: Univ. Science)
Perlman, E. S., et al. 1996, ApJS, 104, 251
Pettersen, B. R. 1989, Sol. Phys., 121, 299
Pettersen, B. R., Cochran, A. L., & Barker, E. S. 1985, AJ, 90, 11
Pettersen, B. P., & Hawley, S. L. 1989, A&A, 217, 187
Petit, M. 1980, Inf. Bull. Variable Stars, No. 1788
———. 1990, A&AS, 85, 971
Pye, J. P., et al. 1995, MNRAS, 274, 1165
Rodonó, M. 1978, A&A, 66, 175
Rucinski, S. M., & Lim, J. 1994, in ASP Conf. Ser. 64, Cool Stars, Stellar Systems, and the Sun: Eighth Cambridge Workshop, ed. J.-P. Caillault (San Francisco: ASP), 462
Rumph, T., Bowyer, S., & Vennes, S. 1994, AJ, 107, 2108
Russell, J. L., Lasker, B. M., McLean, B. J., Sturch, C. R., & Jenkner, H. 1990, AJ, 99, 2059
Schachter, J. F., et al. 1993, ApJ, 412, 541
Schmidt, G. D., Bergeron, P., Liebert, J., & Saffer, R. A. 1992, ApJ, 394, 603
Schmidt, M., & Green, R. F. 1983, ApJ, 269, 352
Sion, E. M., Greenstein, J. L., Landstreet, J. D., Liebert, J., Shipman, H. L., & Wegner, G. A. 1983, ApJ, 269, 253
Stark, A. A., Gammie, C. F., Wilson, R. W., Bally, J., Linke, R. A., Heiles, C., & Hurwitz, M. 1992, ApJS, 79, 77
Vennes, S., Bowyer, S., & Dupuis, J. 1996a, ApJ, 461, L103
Vennes, S., Polomski, E., Bowyer, S., & Thorstensen, J. R. 1995, ApJ, 448, L9
Vennes, S., Thejll, P., Wickramasinghe, D. T., & Bessell, M. S. 1996b, ApJ, 467, 782
Voges, W., et al. 1997, A&A, in press
Walter, R., & Fink, H. H. 1993, A&A, 274, 105
Weedman, D. W. 1973, ApJ, 183, 29
———. 1977, ARA&A, 15, 69
Weiler, K. W., & Johnston, K. J. 1980, MNRAS, 190, 269
White, S. M., Pallavicini, R., & Kundu, M. R. 1992, Mem. Soc. Astron. Italiana, 63, 751
Wilkes, B. J., & Elvis, M. 1987, ApJ, 323, 243
Wood, M. 1995, in Lecture Notes in Physics, 443, White Dwarfs, ed. D. Koester & K. Werner (Berlin: Springer), 41